Scanning electrochemical cell microscopy: High-resolution structure−property studies of mono- and polycrystalline electrode materials

Enrico Daviddi,[1] *Lachlan F. Gaudin,*[2] *and Cameron L. Bentley*[2,*]

[1]Department of Chemistry, University of Warwick, Coventry CV4 7AL, U.K.
[2]School of Chemistry, Monash University, Clayton, Victoria 3800, Australia

*Corresponding author, email: cameron.bentley@monash.edu

ABSTRACT. Scanning electrochemical cell microscopy (SECCM) is a nanopipette-based scanning electrochemical probe microscopy technique that utilises a mobile droplet cell to measure and visualise electrode activity with high spatiotemporal resolution. This article spotlights the use of SECCM for studying the electrochemistry of crystalline electrode materials, ranging from well-defined monocrystals (*e.g.*, transition metal dichalcogenides: MoS_2, WS_2 and WSe_2) to structurally/compositionally heterogeneous polycrystals (*e.g.*, polycrystalline Pt, Au, Pd, Cu, Zn, low carbon steel, boron-doped diamond) and covering the diverse areas of (photo)electrocatalysis, corrosion science, surface science and electroanalysis. In particular, it is emphasised how nanoscale-resolved information from SECCM is readily related to electrode structure and properties, collected at a commensurate scale with complementary, co-located microscopy/spectroscopy techniques, to allow structure−property relationships to be assigned *directly* and *unambiguously*.

1. INTRODUCTION

It is well-established that the kinetics and mechanisms of complex (*e.g.*, inner-sphere) electrochemical processes are strongly influenced by electrode structure and composition. All solid electrode surfaces—from the simplest monocrystals to the most complex composite nanomaterials—possess some degree of structural or compositional heterogeneity, which can be readily observed using a suite of routine high-resolution microscopy and/or spectroscopy methods. Such heterogeneity is often seen to affect electrochemical behaviour; however, the macroscopic "bulk" techniques conventionally used in electrochemistry only provide the surface "weighted average" response of the entire electrode, making it difficult to unambiguously attribute a desirable property (*e.g.*, electrochemical activity, selectivity, stability *etc.*) to a specific surface structural motif (*e.g.*, crystallographic orientation, elemental composition, presence of defects, nanoparticle size *etc.*). Thus, with electrosynthesis experiencing a "renaissance" [1] and the increasing uptake of electrochemical technologies in

green energy storage and conversion [2], there has arguably never been a more important time to develop techniques that can measure electrode activity at the scale of microscopic surface heterogeneities (*i.e.*, nm – μm scale).

There is an expanding toolbox of electrochemical techniques that are capable of probing and (ideally) imaging electrodes and electrode processes at the (sub-)microscale, as summarised in a recent review on the topic [3]. Among these techniques, this article considers the merits of scanning electrochemical cell microscopy (SECCM) [4] for this endeavour. In SECCM, a fluidic nanopipette probe is used to carry out local electrochemistry within a confined region of an electrode surface, with a spatial-resolution (down to tens-of-nm [5, 6]) defined by the area of meniscus contact. Activity and substrate topography are measured synchronously (*in situ*) to provide high-resolution electrochemical and topographical "maps" (or dynamic movies) that can be readily cross-correlated with co-located microscopy/spectroscopy to unambiguously assign electrode structure−property relationships [7]. Further details on the technical development, operational principles, feedback types, and imaging modes of SECCM can be found elsewhere [3, 8].

This article follows on from two previous contributions to *Curr. Opin. Electrochem.*, which showcased the use of SECCM for high spatiotemporal resolution measurements on versatile electrode substrates [9] and the electrochemical interrogation of single-entities [10]. The scope of this article is limited to structure−property mapping of electrode surfaces, highlighting key advances since 2017 (*i.e.*, when Ref [9] was published). Herein, discussions are focused on crystalline electrode materials, including well-defined monocrystals (single-crystals) of long-range order (*e.g.*, layered materials) and extended surfaces of structurally/compositionally heterogeneous polycrystals (*e.g.*, polycrystalline metals). Note that ensemble-type electrodes (*e.g.*, nanoparticles on an electrode support) are not covered here, as they were the focus of a recent minireview [11].

2. MONOCRYSTALLINE ELECTRODE MATERIALS

Monocrystals (*e.g.*, metal single crystals or layered materials), prepared to display a particular surface orientation, are traditionally utilised in electrochemistry to elucidate the role of surface structure in modulating electrochemical activity [12]. They represent the "simplest" class of electrode material, and yet even apparently monocrystalline surfaces may exhibit structural heterogeneities across length scales (*e.g.*, step edges, atomic vacancies, mechanical strain *etc.*), depending on the way that they are produced. This was showcased in a series of pioneering SECCM studies on sp^2 carbon materials, notably graphite and graphene, which were predominantly carried out between 2012 and 2015 [13]. As discussed below, monocrystalline (photo)electrocatalysts and semiconductor photoelectrodes, mainly based on the transition metal dichalcogenides (TMDs), have been the subject of more recent SECCM studies.

Monocrystalline electrocatalysts. Many studies have reported that the edge plane is solely responsible for the electrocatalytic activity of bulk TMD crystals, with some authors going as far as calling the basal planes "inactive" or "catalytically inert" [14], typically inferred indirectly from macroscopic electrochemical data alone. Enhanced hydrogen evolution reaction (HER) activity was directly visualised at the step edges of bulk molybdenite crystals (2H-MoS_2) for the first time through correlative SECCM-atomic force microscopy (AFM) studies, as shown in Figure 1A. In addition, the "catalytically inert" basal plane theory was also debunked, with local Tafel measurements revealing an exchange current density comparable to Au or Ni [5, 15, 16]. Further work on bulk crystals of molybdenite (2H-MoS_2) and tungstenite (2H-WS_2) [17], as well as synthesised nanosheets of 1H-MoS_2 [6], also demonstrated that electrocatalytic activity varies from basal surface to basal surface, or even within a single basal plane (μm-scale), attributed to mechanical deformation, structural defects or surface aging affecting the local electronic structure.

Another factor that may influence the activity of monocrystalline electrocatalysts is variations in surface elemental composition, as highlighted by local voltammetric studies on complex iron nickel sulfide (nominally $Fe_{4.5}Ni_{4.5}S_8$) crystals. While all monocrystals were {111} orientated, slight changes in the Fe/Ni/S ratio due to the material synthesis conditions were shown to cause a dramatic change in both the shape of the voltammetric curve (related to surface redox transformations of the electrocatalyst) and HER overpotential (*i.e.*, HER kinetics). In general, the most active surfaces were the ones with the highest proportions of Fe relative to Ni [18].

Monocrystalline photoelectrodes. TMDs are also promising materials for optoelectronic applications, especially as atomically-thin layers, and therefore it is important to understand their photo-induced charge-transfer properties. SECCM enabled the characterisation of TMDs with high lateral resolution, highlighting the local effect of crystal thickness (*i.e.*, number of layers), surface defects, and step edges on photocatalytic activity and parasitic charge recombination [19-21]. In particular, multi-layer step edges were shown to inhibit photoinduced charge-transfer by functioning as recombination centres in thin layers of *p*-type WSe_2 [19]. In a follow-up study, a novel Carrier Generation-Tip Collection (CG-TC) mode of SECCM confirmed the detrimental role of step edges as recombination centres, as shown in Figure 1B, and further revealed highly anisotropic charge carrier transport within *n*-type WSe_2, with the in-plane hole diffusion length being approximately 3 orders-of-magnitude larger than the out-of-plane [20].

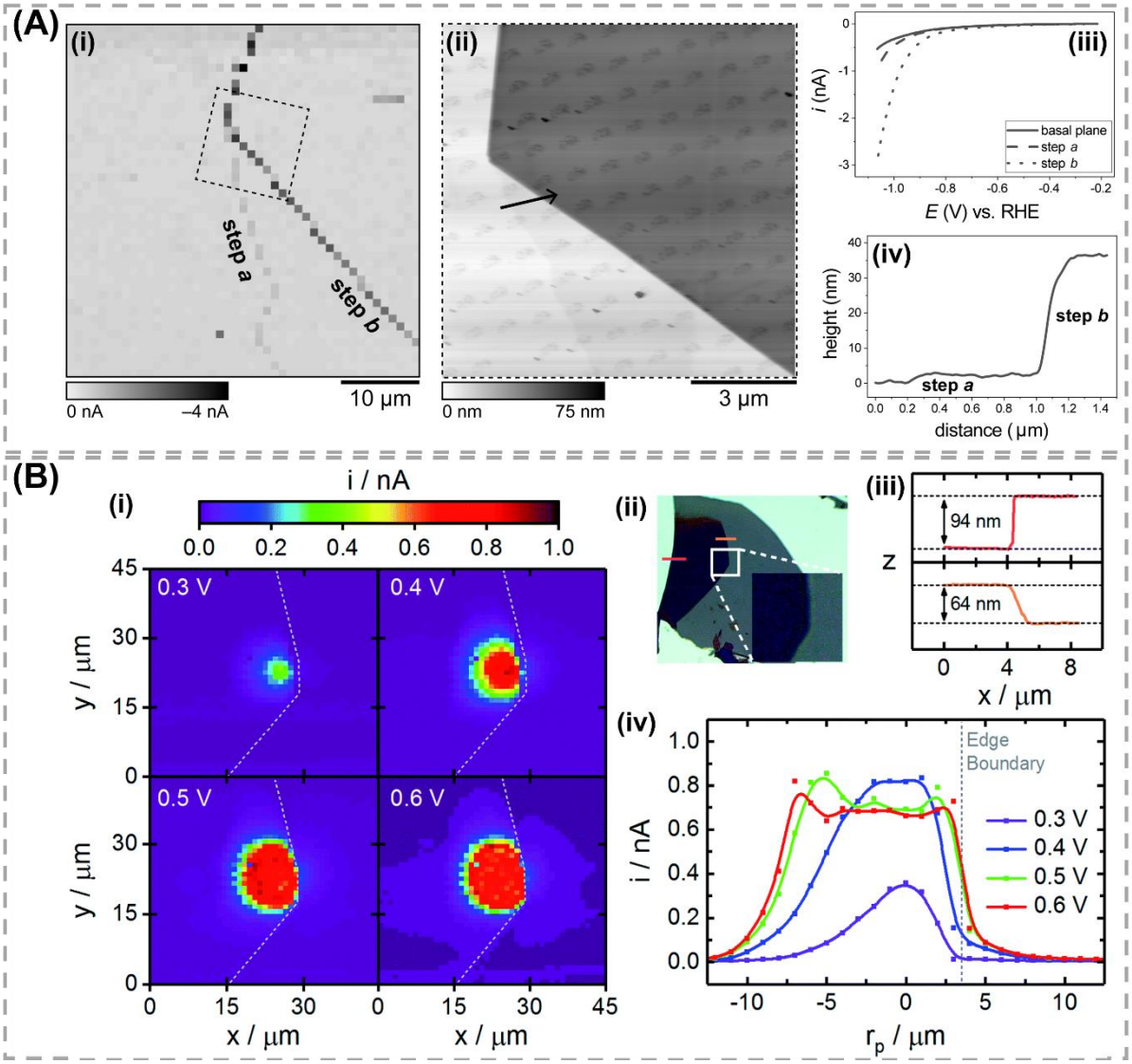

Figure 1. Local electrocatalytic and photoelectrochemical activity of monocrystalline TMDs. (A) HER on a mechanically-exfoliated natural molybdenite crystal (2H-MoS_2) surface, showing enhanced electrocatalytic activity at step edges. **(i)** Electrochemical map (scan area = 45 × 45 μm^2; hopping distance = 1 μm) obtained at −1.05 V vs. RHE in a 0.1 M $HClO_4$ solution. **(ii)** AFM topographical image of the area indicated by dashed box in (i). **(iii)** Representative linear sweep voltammograms (LSVs) obtained from the basal plane and steps *a* and *b* [labelled in (i)], with voltammetric scan rate, υ = 0.25 V s^{-1}. **(iv)** AFM line profile of area indicated by arrow shown in (ii). Adapted from Ref [15] with permission from The Royal Society of Chemistry. **(B)** CG-TC SECCM imaging of a *n*-type WSe_2 crystal, illuminated locally with a 633 nm Gaussian beam (approximately centred in each of the images). **(i)** Photoelectrochemical maps (scan area = 45 × 45 μm^2; hopping distance = 1 μm) obtained from the photo-oxidation of I^- (potentials vs. Ag/AgI). The white dotted line indicates the position of a step/edge feature of *ca*. 64 nm height. **(ii)** Optical transmission image of the WSe_2 crystal, showing the location of the step/edge feature in (i). **(iii)** AFM line profiles obtained at the lines indicated in (ii). **(iv)** Cross sections of the SECCM photocurrent images shown in (i). Adapted from Ref [20] with permission from The Royal Society of Chemistry.

3. POLYCRYSTALLINE ELECTRODE MATERIALS

Electrodes of practical importance are often designed to be structurally and/or compositionally heterogeneous. A polycrystalline metal electrode is arguably the most well-known example of this, possessing surfaces with many degrees of structural (*e.g.*, grains of different crystallographic orientation and grain boundaries, GBs) and compositional (*e.g.*, presence of surface oxides, intermetallic inclusions *etc.*) heterogeneity. The *pseudo single-crystal approach* [22] was introduced to study structure-dependent electrochemical activity of polycrystalline metal electrodes, in which SECCM is used to electrochemically interrogate individual grains (crystallites) and GBs, which are structurally characterised *ex situ* with co-located electron backscattered diffraction (EBSD). While early studies making use of this approach focused predominantly on polycrystalline Pt (poly-Pt) [22-25], more recently it has been expanded to investigate a range of different materials, which, as discussed below, encompass the diverse areas of electrocatalysis, corrosion science, surface science and electroanalysis. In addition, it is also worth acknowledging the growing body of work on the local nucleation and growth gas nanobubbles on crystalline electrode materials (MoS_2, Au, Pt) [26-28], which will not be discussed in detail here.

Polycrystalline metal electrocatalysts. The inner-sphere I^-/I_2 process is well-known to proceed in two-steps *via* a stable I_3^- intermediate in aprotic solvents such as propylene carbonate (PC). Indeed, the I^-/I_3^- couple is the most commonly employed redox mediator system in dye-sensitised solar cells, where the I_3^-/I^- process usually takes place at a platinised counter electrode. For this reason, a recent SECCM study considered the surface structure-dependent kinetics of the I^-/I_2 process on poly-Pt in a PC-based electrolyte system (*n.b.* guidelines for the use of non-aqueous electrolytes in SECCM were also reported, therein). Each redox process, I^-/I_3 and I_3^-/I_2, presented a different grain-dependent activity, as shown in Figure 2A, especially on highly-stepped (high-index) surfaces, suggesting a preference for different active sites.

Furthermore, the I_3^-/I_2 process exhibited accelerated kinetics in the presence of elevated surface misorientation, which was observed within and around some grains, shown in Figure 2B [29].

Further work on poly-Pt included the local measurement of the potential of zero charge (PZC), achieved by monitoring changes in the potential-dependent double layer charging current. A general trend in the PZC with the grain orientation was derived, with grains closer to {111} having more positive PZCs and grains closer to {100} or {110} having more negative PZCs. Furthermore, the authors noted an apparently negative correlation between PZC and the Tafel slope associated with the HER: higher PZC values corresponded with lower Tafel slope values and higher electrocatalytic activities (*i.e.*, higher catalytic currents) [30].

As highlighted in a recent review [31], correlative SECCM-EBSD has been used to spatially-resolve the nanoscale catalytic active sites for the electrocatalytic CO_2 reduction reaction (eCO_2RR) on poly-Au. Macroscopic electrochemistry revealed that the faradaic efficiency for CO production decreased with increasing average grain size, which was attributed to a decreasing GB density, suggesting that GBs are a catalytic active site for the eCO_2RR. To confirm this hypothesis, SECCM line-scans were performed across different GBs, providing the first direct evidence of enhanced eCO_2RR activity on/at the boundary region. Such enhancement was highly reaction dependent, and was not observed for the competing HER [32]. In a follow-up study, technical improvements in SECCM (both in terms of spatial-resolution and number of measurements) coupled with co-located high-resolution EBSD revealed that the enhanced eCO_2RR activity is not due to the lattice strain associated with active GBs (as originally proposed in reference [32]) but rather from the presence of surface-terminating dislocations. The dislocation density was shown to be elevated at surface defects such as GBs and slip bands and could also be introduced by mechanically straining the surface (*i.e.*, inducing misorientation), as demonstrated in Figure 2C [33].

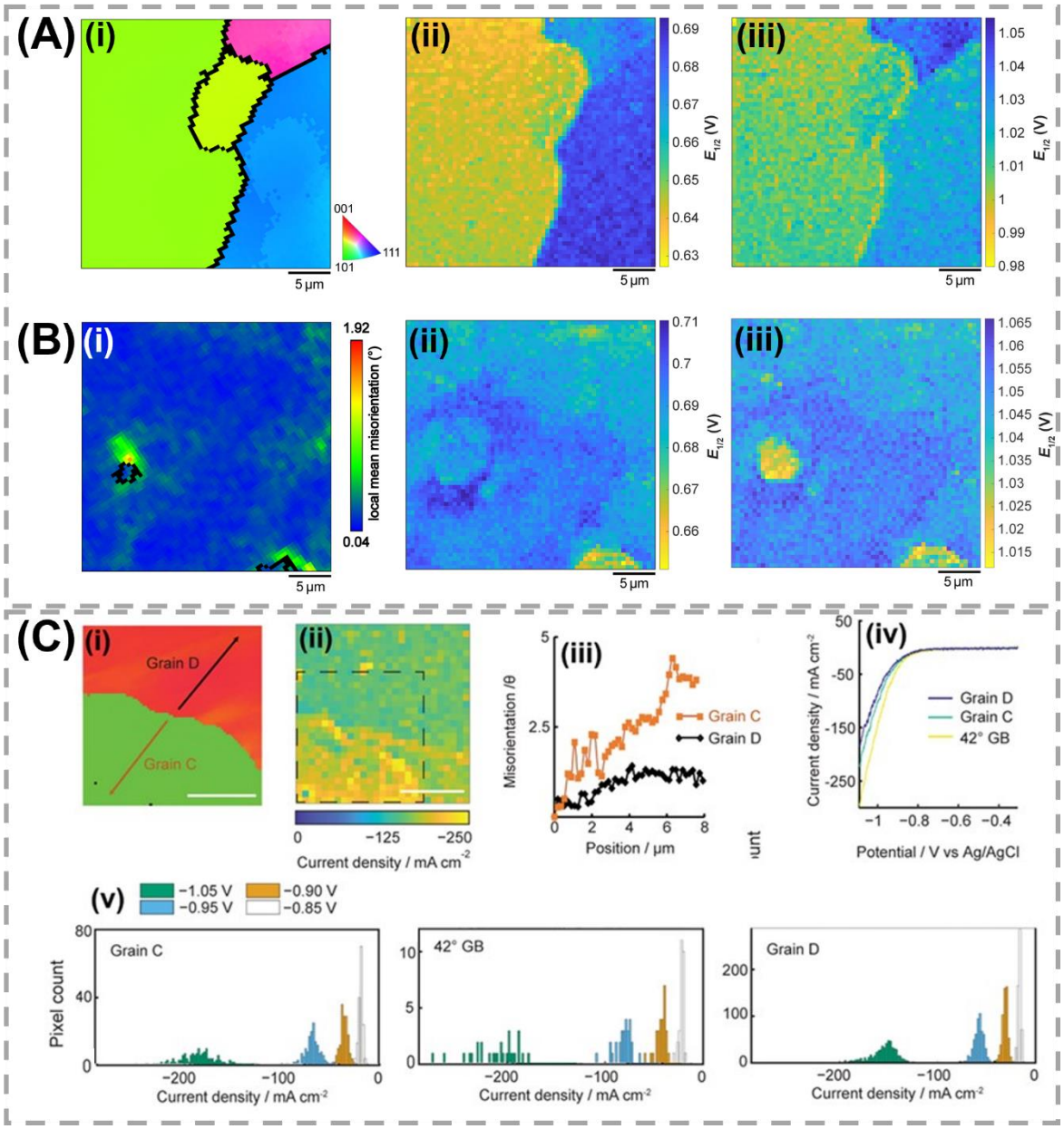

Figure 2. Structure-dependent electrocatalytic activity of polycrystalline metal electrodes. (A) Correlative structure–activity mapping of the I^-/I_2 process in propylene carbonate at poly-Pt. Co-located maps of **(i)** crystallographic orientation (from EBSD) and half-wave potentials ($E_{1/2}$) associated with the **(ii)** I^-/I_3^- and **(iii)** I_3^-/I_2 processes (from SECCM). **(B)** Co-located maps of **(i)** local mean misorientation (from EBSD) and $E_{1/2}$ values associated with the **(ii)** I^-/I_3^- and **(iii)** I_3^-/I_2 processes (from SECCM). The following parameters were used during SECCM: scan area = 29 × 29 µm^2; hopping distance = 0.5 µm. Adapted with permission from Ref [29]. Copyright 2020 American Chemical Society. **(C)** Correlative structure–activity mapping of the eCO_2RR at poly-Au. Co-located maps of **(i)** crystallographic orientation (from EBSD) and **(ii)** electrochemical activity (from SECCM, obtained at −1.05 V vs. Ag/AgCl under an atmosphere of CO_2; scan area = 13.5 × 14 µm^2; hopping distance = 0.5 µm). **(iii)** Linear misorientation profiles of the lines shown in (i). **(iv)** Representative LSVs (υ = 0.5 V s^{-1}) extracted from the two grains, and the GB region [labelled in (i)]. **(v)** Histograms of current density, extracted from all pixels of the map in (ii), separated by region of pixel, and colour coded according to applied potential. Adapted by permission from Ref [33]. Copyright 2021, Macmillan Publishers Ltd.

Corrosion of polycrystalline metals. The "oil-immersed" variant of SECCM was recently introduced to study relatively slow corrosion-related processes in a three-phase metal|aqueous nanodroplet|oil setup. In this configuration, a thin layer of oil is applied to the investigated substrate, which improves the stability of the droplet cell over prolonged mapping times (necessary to accurately measure the local corrosion potential [34]) and allows for the study of corrosion under industrially relevant conditions [35]. This approach was employed to investigate the corrosion properties of a complex Al alloy (AA7075-T73) under a three-phase $metal_{(s)}|NaCl_{(aq)}|oil_{(l)}$ environment. Spatially-resolved measurements of the corrosion potential and corrosion current revealed a strong correlation with the surface composition: Fe-rich constituent phases (and inclusions) were more susceptible to (galvanic) corrosion [34].

SECCM has also been used to study the corrosion susceptibility of other alloys under acidic conditions, including low carbon steel [36-38], as well as pure metals such as poly-Zn [39] and poly-Cu [35]. The body of work carried on low carbon steel, exemplified in Figure 3A, is indicative of how it is possible to obtain information on the unique grain-dependencies of the various corrosion-related processes in a single experiment, such as active iron dissolution (Figure 3A-ii) and passive film formation/reduction (Figure 3A-iii). In addition, the high spatial-resolution achievable by SECCM allowed for the exploration of single MnS inclusions, which exhibited elevated anodic (shown in Figure 3A-iv to 3A-vi) [38] and cathodic activity [37]. Similar work was carried out on poly-Zn [39], which set the stage for a more comprehensive analysis of grain-dependent processes.

Indeed, while the work on low carbon steel and poly-Zn showcased the potential of the pseudo single-crystal approach in the field of corrosion [36-39], it was the more recent work on poly-Cu that pushed the grain-dependent analysis towards being systematic, covering the entire spectrum of crystallographic orientations [35]. This is demonstrated in Figure 3B for the Cu oxidation reaction (similar analysis was performed for the oxygen reduction and Cu

deposition processes), where electrochemical activity data were obtained from the SECCM image (Figure 3B-i) and cross-correlated to surface structural information (Figure 3B-ii) in a two-dimensional plot, rather than solely focussing on the low-index facets (*e.g.*, Figure 3B-iii), as in Refs [36-39]. Figure 3B-iv displays a complex pattern of surface activity (corrosion susceptibility/resistance) and highlights the important role of grains of high-index orientation, which each possessed unique electrochemical activities that could not be predicted simply through a combination of the low-index {001}, {011}, and {111} responses [35].

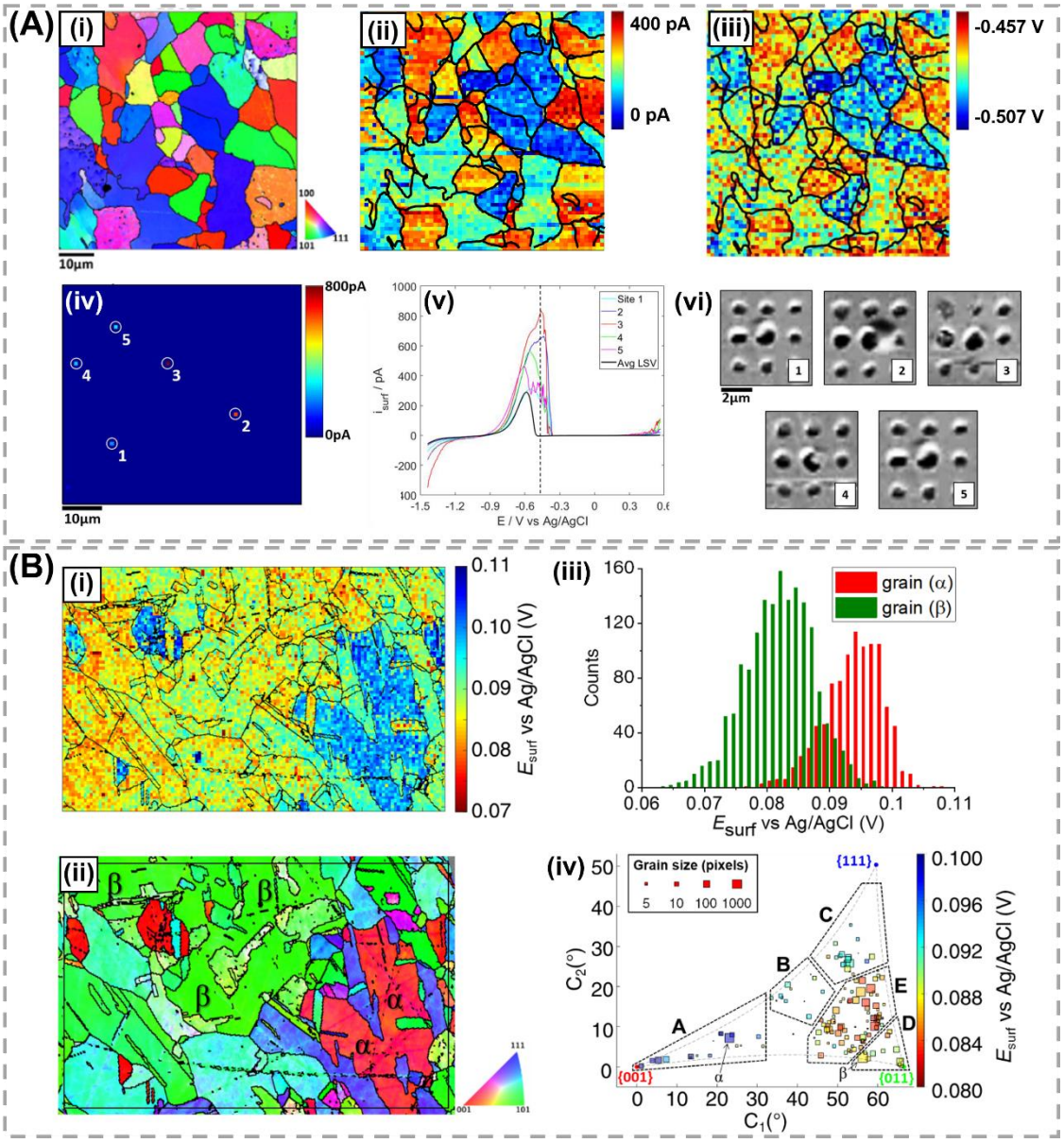

Figure 3. Spatially-resolved corrosion studies on polycrystalline metals. (A) Grain-dependent corrosion-related processes associated with low carbon steel in 0.005 M H_2SO_4. Co-located maps of **(i)** crystallographic orientation (from EBSD) and **(ii)** peak current associated with iron dissolution and **(iii)** peak potential associated with passive film reduction (from SECCM). **(iv)** Surface current map obtained at −0.447 V vs. Ag/AgCl, with active pixels labelled. **(v)** LSVs (υ = 2 V s^{-1}) extracted from the five highly active pixels labelled in (iv) versus the average response (black trace) obtained from all pixels. **(vi)** SEM images of the active pixels (centre) indicated in (iv) and eight adjacent pixels. The following parameters were used for (ii) − (iv): scan area = 72 × 72 μm^2; hopping distance = 1.2 μm. Adapted from Ref [38], Copyright 2020, with permission from Elsevier. **(B)** Grain-dependent Cu dissolution at poly-Cu (immersed in dodecane) in 0.01 M H_2SO_4. Co-located maps of **(i)** surface potential (from SECCM; applied current density = +6.25 mA cm^{-2}; scan area = 127 × 81 μm^2; hopping distance = 1 μm) and **(ii)** crystallographic orientation (from EBSD; grains labelled α and β are representative of the {001} and {011} orientations, respectively). **(iii)** Histogram of surface potential values extracted from grains α and β. **(iv)** Grain orientation correlation analysis of surface potentials extracted from (i) versus the average grain orientation from (ii). Location in the *xy* axes indicates orientation, whilst colour indicates potential. Reprinted from Ref [35] with permission from The Royal Society of Chemistry.

Surface processes at polycrystalline noble metals. In contrast to the active metals discussed above (*e.g.*, poly-Zn), noble metals do not corrode in non-oxidising acids (*e.g.*, dilute sulfuric acid) and instead often exhibit well-defined surface processes that are characteristic for a specific metal/electrolyte combination. For example, in the absence of oxygen (achieved by carrying out SECCM in a specially-designed environmental cell [40]), poly-Pd exhibited well-defined oxide formation (Figure 4A-ii), oxide stripping (Figure 4A-iii) and hydrogen adsorption-absorption (Figure 4A-iv) processes, which each possessed unique surface structure dependencies, as shown in Figure 4A. Interestingly, as shown in Figure 4B, apparently higher electrochemical activity was observed at particular GBs, which was shown to coincide with areas of high physical surface deformation, induced during the surface preparation of poly-Pd through flame annealing followed by rapid quenching [41].

Electroanalysis at non-metal polycrystals. Metals are not the only type of material that can be analysed using the pseudo single crystal approach; conductive boron-doped diamond (BDD) is an sp^3 carbon material that is widely used in its polycrystalline form for electroanalysis and electrochemical sensing. The grain-dependent behaviour of poly-BDD was the object of one of the first SECCM studies, which found that the heterogeneous electron-transfer rate for outer-sphere, inner-sphere and complex multistage electrochemical reactions increases with the surface boron-dopant concentration, which in turn depends on the crystallographic orientation [42]. Similar observations were recently made on as-grown (*i.e.*, not further polished) poly-BDD, shown in Figure 4C, which presented mainly two surface facets: {111}, which was more-doped and more active and; {100}, which was less-doped and less active, especially in its oxygen-terminated form [43]. The same also holds true for the electrochemical window of poly-BDD electrodes, which was shown to be narrower on more highly-doped surfaces, owing to an increased electrocatalytic activity towards solvent/electrolyte electrolysis [44].

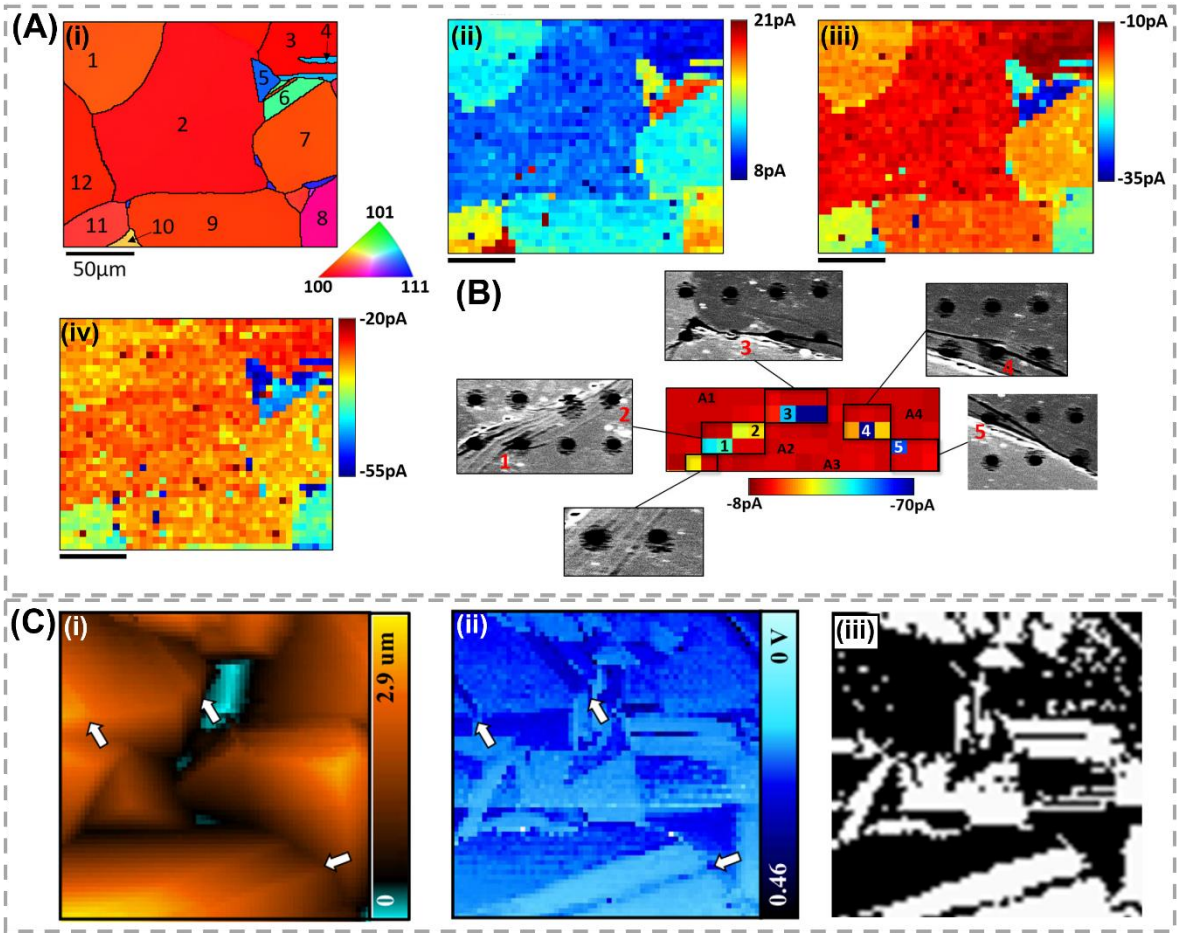

Figure 4. Structure-dependent surface processes and redox activity of polycrystalline electrodes. **(A)** Structure-dependent surface processes of poly-Pd in 0.5 M H_2SO_4. Co-located maps of **(i)** crystallographic orientation (from EBSD) and electrochemical activity maps of the: **(ii)** palladium oxide (PdO_x) formation; **(iii)** PdO_x reduction and; **(iii)** hydrogen adsorption-absorption processes (from SECCM; scan area = 200 × 175 µm^2; hopping distance = 5 µm), obtained at +0.7 V, +0.2 V and −0.45 V vs. Ag/AgCl, respectively. **(B)** Electrochemical activity map (hopping distance = 4 µm) obtained from an apparently active grain boundary of poly-Pd at −0.4 V vs. Ag/AgCl, alongside SEM images of indicated sites. Adapted from Ref [41], Copyright 2020, with permission from Elsevier. **(C)** Grain-dependent electrochemical activity of (hydrogen-terminated) poly-BDD towards the $[Fe(CN)_6]^{4-/3-}$ process. SECCM **(i)** topography and **(ii)** $E_{1/2}$ maps (scan area = 10 × 10 µm^2; hopping distance = 156.25 nm). **(iii)** Binarisation image of the {100} (black) and {111} (white) facets, derived from (ii). Adapted with permission from Ref [43]. Copyright 2021 American Chemical Society.

4. Conclusions and Outlook

There has never been a greater need for techniques that can probe/characterise electrochemical fluxes and/or electrode activity on a commensurate scale to microscopic surface structural heterogeneities (*i.e.*, nm – μm scale). This article has sought to demonstrate the merits of SECCM for this purpose, highlighting recent studies on extended surfaces of crystalline electrode materials. Studies on well-defined monocrystalline electrode materials (*e.g.*, TMDs) revealed the important role of step edges, for example as beneficial catalytic active sites or detrimental recombination centres, in modulating macroscopic (photo)electrochemical activity. Studies on structurally/compositionally heterogeneous polycrystalline electrode materials showcased the unique electrochemical activities of the constituent crystallites (grains) and further highlighted the role of GBs and inclusions as active sites for electrocatalytic and corrosion-related processes. All discussed studies emphasised the importance of correlative multi-microscopy in structure−property studies, whereby nanoscale-resolved electrochemical data from SECCM is cross-correlated with co-located structural information from complementary high-resolution spectroscopy/microscopy (*e.g.*, AFM, SEM, EBSD *etc.*).

Looking to the future, technical developments will undoubtedly see continuing improvements in terms of the spatial-resolution and imaging speed, as well as increasing capability to combine SECCM with other forms of microscopic analysis, ideally *in situ*. From a materials perspective, there are almost limitless possibilities for SECCM, both for the structure−property studies focused herein, as well as for high-throughput materials synthesis [40] and screening [45] approaches. Future studies may target the ever-growing library of monocrystalline layered (two-dimensional) materials or more complex, multi-elemental and/or multi-phase polycrystalline materials (*e.g.*, alloys), which are finding increasing applications in electrochemical science. All-in-all, SECCM has firmly cemented itself as a premier tool for

microscopic structure−property studies and will no doubt play an important role in the guided discovery, design, and engineering of novel electrode materials, moving forward.

ACKNOWLEDGEMENTS

E.D. thanks the Engineering and Physical Sciences Research Council (EPSRC) of the British Government for support (grant reference EP/V047981/1). C. L. B. is the recipient of an Australian Research Council (ARC) Discovery Early Career Researcher Award (DECRA, project number DE200101076), funded by the Australian Government.

REFERENCES

1. Yan M, Kawamata Y, Baran PS: **Synthetic Organic Electrochemical Methods Since 2000: On the Verge of a Renaissance.** *Chem. Rev.* 2017, **117**:13230-13319.

2. Seh ZW, Kibsgaard J, Dickens CF, Chorkendorff I, Nørskov JK, Jaramillo TF: **Combining Theory and Experiment in Electrocatalysis: Insights into Materials Design.** *Science* 2017, **355**:146.

3. Bentley CL, Edmondson J, Meloni GN, Perry D, Shkirskiy V, Unwin PR: **Nanoscale Electrochemical Mapping.** *Anal. Chem.* 2019, **91**:84-108.

4. Ebejer N, Schnippering M, Colburn AW, Edwards MA, Unwin PR: **Localized high resolution electrochemistry and multifunctional imaging: scanning electrochemical cell microscopy.** *Anal. Chem.* 2010, **82**:9141-5.

5. Bentley CL, Kang M, Unwin PR: **Nanoscale Structure Dynamics within Electrocatalytic Materials.** *J. Am. Chem. Soc.* 2017, **139**:16813-16821.

6. Takahashi Y, Kobayashi Y, Wang Z, Ito Y, Ota M, Ida H, Kumatani A, Miyazawa K, Fujita T, Shiku H, Korchev YE, Miyata Y, Fukuma T, Chen M, Matsue T: **High-Resolution Electrochemical Mapping of the Hydrogen Evolution Reaction on Transition-Metal Dichalcogenide Nanosheets.** *Angew. Chem. Int. Ed.* 2020, **59**:3601-3608.

7. Bentley CL, Kang M, Unwin PR: **Nanoscale Surface Structure-Activity in Electrochemistry and Electrocatalysis.** *J. Am. Chem. Soc.* 2019, **141**:2179-2193.

8. Ebejer N, Guell AG, Lai SC, McKelvey K, Snowden ME, Unwin PR: **Scanning electrochemical cell microscopy: a versatile technique for nanoscale electrochemistry and functional imaging.** *Annu. Rev. Anal. Chem.* 2013, **6**:329-51.

9. Bentley CL, Kang M, Unwin PR: **Scanning Electrochemical Cell Microscopy: New Perspectives on Electrode Processes in Action.** *Curr. Opin. Electrochem.* 2017, **6**:23-30.

10. Wahab OJ, Kang M, Unwin PR: **Scanning Electrochemical Cell Microscopy: A Natural Technique for Single Entity Electrochemistry.** *Curr. Opin. Electrochem.* 2020, **22**:120-128.

11. Bentley CL: **Scanning electrochemical cell microscopy for the study of (nano)particle electrochemistry: From the sub‐particle to ensemble level.** *Electrochemical Science Advances* 2021, DOI: 10.1002/elsa.202100081.

12. O'Mullane AP: **From single crystal surfaces to single atoms: investigating active sites in electrocatalysis.** *Nanoscale* 2014, **6**:4012-4026.

13. Unwin PR, Guell AG, Zhang G: **Nanoscale Electrochemistry of sp^2 Carbon Materials: From Graphite and Graphene to Carbon Nanotubes.** *Acc. Chem. Res.* 2016, **49**:2041-2048.

14. Benck JD, Hellstern TR, Kibsgaard J, Chakthranont P, Jaramillo TF: **Catalyzing the Hydrogen Evolution Reaction (HER) with Molybdenum Sulfide Nanomaterials.** *ACS Catal.* 2014, **4**:3957-3971.

15. Bentley CL, Kang M, Maddar FM, Li F, Walker M, Zhang J, Unwin PR: **Electrochemical maps and movies of the hydrogen evolution reaction on natural crystals of molybdenite (MoS_2): basal vs. edge plane activity.** *Chem. Sci.* 2017, **8**:6583-6593.

16. Bentley CL, Unwin PR: **Nanoscale Electrochemical Movies and Synchronous Topographical Mapping of Electrocatalytic Materials.** *Faraday Discuss.* 2018, **210**:365-379.

17. Tao B, Unwin PR, Bentley CL: **Nanoscale Variations in the Electrocatalytic Activity of Layered Transition-Metal Dichalcogenides.** *J. Phys. Chem. C* 2019, **124**:789-798.

18. Bentley CL, Andronescu C, Smialkowski M, Kang M, Tarnev T, Marler B, Unwin PR, Apfel UP, Schuhmann W: **Local Surface Structure and Composition Control the Hydrogen Evolution Reaction on Iron Nickel Sulfides.** *Angew. Chem. Int. Ed.* 2018, **57**:4093-4097.

19*. Hill JW, Hill CM: **Directly Mapping Photoelectrochemical Behavior within Individual Transition Metal Dichalcogenide Nanosheets.** *Nano Lett.* 2019, **19**:5710-5716.

Deploys SECCM in tandem with global illumination to investigate the photoactivity of *p*-type WSe_2; crystal thickness (*i.e.*, number of layers) and the presence of defect structures are shown to affect the local rate of photoelectrochemical reactions for both outer sphere and inner sphere redox couples.

20**. Hill JW, Hill CM: **Directly visualizing carrier transport and recombination at individual defects within 2D semiconductors.** *Chem. Sci.* 2021, **12**:5102-5112.

Introduces the CG-TC mode of SECCM and uses this innovative approach to quantify charge-carrier transport in *n*-type WSe_2 crystals; highly anisotropic hole transport within the basal planes is revealed and step edge defects are identified as detrimental charge recombination sites.

21. Tolbert CL, Hill CM: **Electrochemically probing exciton transport in monolayers of two-dimensional semiconductors.** *Faraday Discuss.* 2021, DOI: 10.1039/D1FD00052G.

22. Aaronson BD, Chen CH, Li H, Koper MT, Lai SC, Unwin PR: **Pseudo-single-crystal electrochemistry on polycrystalline electrodes: visualizing activity at grains and grain boundaries on platinum for the Fe^{2+}/Fe^{3+} redox reaction.** *J. Am. Chem. Soc.* 2013, **135**:3873-3880.

23. Aaronson BD, Lai SC, Unwin PR: **Spatially resolved electrochemistry in ionic liquids: surface structure effects on triiodide reduction at platinum electrodes.** *Langmuir* 2014, **30**:1915-1919.

24. Chen CH, Jacobse L, McKelvey K, Lai SC, Koper MT, Unwin PR: **Voltammetric Scanning Electrochemical Cell Microscopy: Dynamic Imaging of Hydrazine Electro-oxidation on Platinum Electrodes.** *Anal. Chem.* 2015, **87**:5782-5789.

25. Chen CH, Meadows KE, Cuharuc A, Lai SC, Unwin PR: **High resolution mapping of oxygen reduction reaction kinetics at polycrystalline platinum electrodes.** *Phys. Chem. Chem. Phys.* 2014, **16**:18545-18552.

26. Wang Y, Gordon E, Ren H: **Mapping the Nucleation of H_2 Bubbles on Polycrystalline Pt via Scanning Electrochemical Cell Microscopy.** *J. Phys. Chem. Lett.* 2019, **10**:3887-3892.

27. Liu Y, Jin C, Liu Y, Ruiz KH, Ren H, Fan Y, White HS, Chen Q: **Visualization and Quantification of Electrochemical H2 Bubble Nucleation at Pt, Au, and MoS_2 Substrates.** *ACS Sensors* 2021, **6**:355-363.

28. Liu Y, Lu X, Peng Y, Chen Q: **Electrochemical Visualization of Gas Bubbles on Superaerophobic Electrodes Using Scanning Electrochemical Cell Microscopy.** *Anal. Chem.* 2021, **93**:12337-12345.

29*. Bentley CL, Kang M, Unwin PR: **Scanning Electrochemical Cell Microscopy (SECCM) in Aprotic Solvents: Practical Considerations and Applications.** *Anal. Chem.* 2020, **92**:11673-11680.

Establishes protocols for the use of non-aqueous electrolytes in SECCM and deploys this technique to investigate the inner-sphere I^-/I_2 process at poly-Pt; grains of specific crystallographic orientation, GBs and areas of high local surface misorientation are identified as potential electrocatalytic "hot spots".

30. Wang Y, Gordon E, Ren H: **Mapping the Potential of Zero Charge and Electrocatalytic Activity of Metal–Electrolyte Interface via a Grain-by-Grain Approach.** *Anal. Chem.* 2020, **92**:2859-2865.

31. Guo SX, Bentley CL, Kang M, Bond AM, Unwin PR, Zhang J: **Advanced Spatiotemporal Voltammetric Techniques for Kinetic Analysis and Active Site Determination in the Electrochemical Reduction of CO2.** *Acc. Chem. Res.* 2022, **55**:241-251.

32. Mariano RG, McKelvey K, White HS, Kanan MW: **Selective increase in CO_2 electroreduction activity at grain-boundary surface terminations.** *Science* 2017, **358**:1187-1192.

33**. Mariano RG, Kang M, Wahab OJ, McPherson IJ, Rabinowitz JA, Unwin PR, Kanan MW: **Microstructural origin of locally enhanced CO_2 electroreduction activity on gold.** *Nat. Mater.* 2021, **20**:1000-1006.

Deploys correlative high-resolution SECCM and EBSD to demonstrate that the locally enhanced eCO_2RR activity at and around GBs on poly-Au electrocatalysts is attributable to the presence of highly active undercoordinated step sites present at surface-terminating dislocations.

34. Li Y, Morel A, Gallant D, Mauzeroll J: **Oil-Immersed Scanning Micropipette Contact Method Enabling Long-term Corrosion Mapping.** *Anal. Chem.* 2020, **92**:12415-12422.

35**. Daviddi E, Shkirskiy V, Kirkman PM, Robin MP, Bentley CL, Unwin PR: **Nanoscale electrochemistry in a copper/aqueous/oil three-phase system: surface structure-activity-corrosion potential relationships.** *Chem Sci* 2020, **12**:3055-3069.

Presents a new data analysis protocols to systematically analyse structure-dependent electrochemical processes across the entire spectrum of crystallographic orientations; deploying this approach to investigate the interrelationship between Cu oxidation, Cu^{2+} deposition and ORR at poly-Cu reveals complex patterns of surface reactivity and highlights the important role of grains of high-index orientation and microscopic surface defects (*e.g.*, microscratches) in modulating corrosion susceptibility/resistance.

36. Yule LC, Bentley CL, West G, Shollock BA, Unwin PR: **Scanning electrochemical cell microscopy: A versatile method for highly localised corrosion related measurements on metal surfaces.** *Electrochim. Acta* 2019, **298**:80-88.

37. Yule LC, Shkirskiy V, Aarons J, West G, Bentley CL, Shollock BA, Unwin PR: **Nanoscale Active Sites for the Hydrogen Evolution Reaction on Low Carbon Steel.** *J. Phys. Chem. C* 2019, **123**:24146-24155.

38. Yule LC, Shkirskiy V, Aarons J, West G, Shollock BA, Bentley CL, Unwin PR: **Nanoscale electrochemical visualization of grain-dependent anodic iron dissolution from low carbon steel.** *Electrochim. Acta* 2020, **332**:135267.

39. Shkirskiy V, Yule LC, Daviddi E, Bentley CL, Aarons J, West G, Unwin PR: **Nanoscale Scanning Electrochemical Cell Microscopy and Correlative Surface Structural Analysis to Map Anodic and Cathodic Reactions on Polycrystalline Zn in Acid Media.** *Journal of The Electrochemical Society* 2020, **167**:041507.

40. Ornelas IM, Unwin PR, Bentley CL: **High-Throughput Correlative Electrochemistry-Microscopy at a Transmission Electron Microscopy Grid Electrode.** *Anal. Chem.* 2019, **91**:14854-14859.

41. Yule LC, Daviddi E, West G, Bentley CL, Unwin PR: **Surface microstructural controls on electrochemical hydrogen absorption at polycrystalline palladium.** *J. Electroanal. Chem.* 2020, **872**:114047.

42. Patten HV, Lai SC, Macpherson JV, Unwin PR: **Active sites for outer-sphere, inner-sphere, and complex multistage electrochemical reactions at polycrystalline boron-doped diamond electrodes (pBDD) revealed with scanning electrochemical cell microscopy (SECCM).** *Anal. Chem.* 2012, **84**:5427-5432.

43*. Ando T, Asai K, Macpherson J, Einaga Y, Fukuma T, Takahashi Y: **Nanoscale Reactivity Mapping of a Single-Crystal Boron-Doped Diamond Particle.** *Anal. Chem.* 2021, **93**:5831-5838.

Deploys SECCM to investigate the $[Ru(NH_3)_6]^{3+/2+}$ and $[Fe(CN)_6]^{4-/3-}$ redox processes at monocrystalline BDD microparticles and (as prepared) poly-BDD electrodes; surface termination (*i.e.*, H-termination vs. O-termination) and crystallographic orientation are shown to strongly influence the electrode kinetics for both processes.

44. Liu DQ, Chen CH, Perry D, West G, Cobb SJ, Macpherson JV, Unwin PR: **Facet‐Resolved Electrochemistry of Polycrystalline Boron‐Doped Diamond Electrodes: Microscopic Factors Determining the Solvent Window in Aqueous Potassium Chloride Solutions.** *ChemElectroChem* 2018, **5**:3028-3035.

45. Banko L, Krysiak OA, Pedersen JK, Xiao B, Savan A, Löffler T, Baha S, Rossmeisl J, Schuhmann W, Ludwig A: **Unravelling Composition–Activity–Stability Trends in High Entropy Alloy Electrocatalysts by Using a Data‐Guided Combinatorial Synthesis Strategy and Computational Modeling.** *Adv. Energy Mater.* 2022, 2103312.